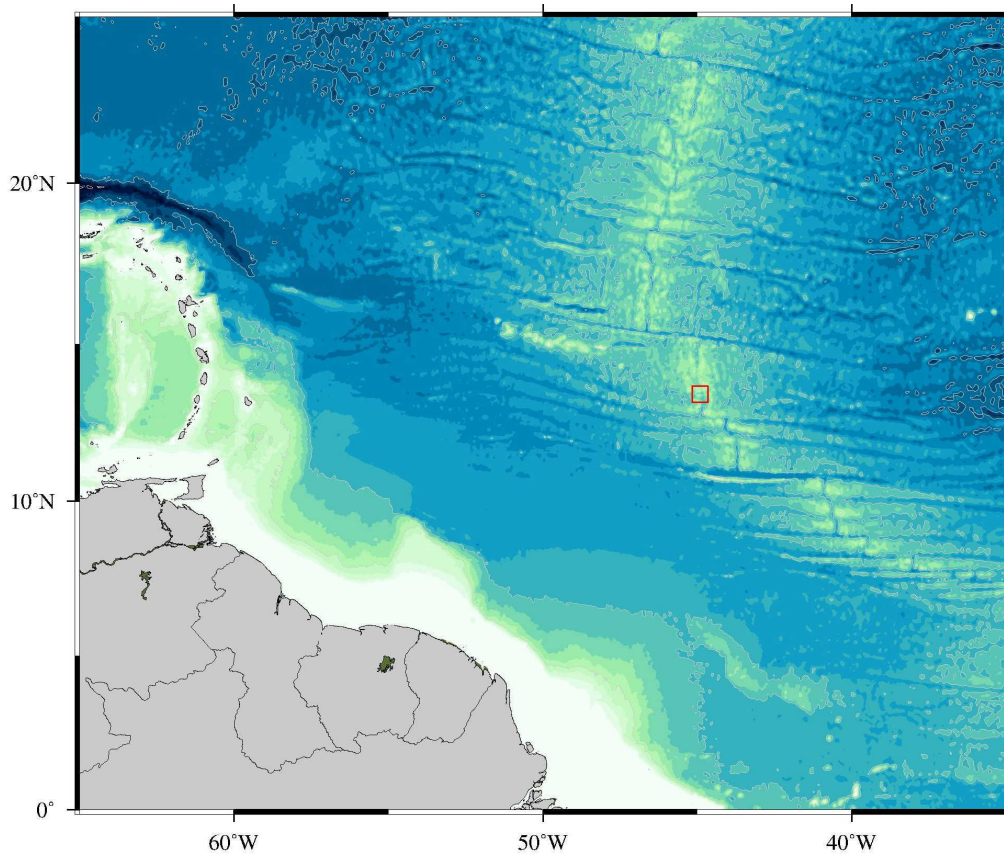


RRS James Cook JC109

Cruise Report

The Role and Extent of Detachment Faulting at Slow-Spreading Mid-Ocean Ridges

Leg 2



11th October – 5th November 2014

Southampton (UK) – Port of Spain (Trinidad)

RRS James Cook JC109

Cruise Report

The Role and Extent of Detachment Faulting at Slow-Spreading Mid-Ocean Ridges

Leg 2

11th October – 5th November 2014
Southampton, UK – Port of Spain, Trinidad



Prof Christine Peirce

**Department of Earth Sciences
University of Durham
South Road
Durham
DH1 3LE**

christine.peirce@durham.ac.uk

November 2014

Table of Contents

Summary	2
1 Background and scientific objectives	2
1.1 Background.....	2
1.2 Study location - 13°N	4
1.3 Scientific objectives.....	5
2 Cruise preparation and mobilisation	7
2.1 Scientific plan.....	7
2.2 Territorial waters and diplomatic clearances	7
2.3 Mobilisation.....	7
2.4 Delays to sailing.....	8
3 Work conducted and data collected	8
3.1 Ocean-bottom seismograph recoveries	9
3.2 Sound velocity profiles	13
3.3 Gravity.....	13
3.4 Swath bathymetry	14
4 Cruise narrative	17
5 Equipment performance	19
5.1 Ocean-bottom seismographs	19
5.2 All other equipment	19
5.3 Ship's machinery and fitted equipment	19
6 Demobilisation	19
Acknowledgements	20
References	20
Tables	21
Table 1 - Way points.....	21
Table 2 - OBS recovery locations	24
Table 3 - Sound velocity profile and acoustic tests.....	25
Table 4 - Gravity base stations.....	25
Table 5 - Scientific personnel	26
Table 6 - Project 13N Principal Scientists, Project Partners and Consultants.....	26



Summary

The primary objective of RRS James Cook cruise JC109 was to recover 25 ocean-bottom seismographs deployed at the 13° 20'N oceanic core complex on the Mid-Atlantic Ridge during JC102, to record local passive micro-seismicity over a period of approximately six months. Gravity and swath bathymetry data were also acquired port-to-port, with the gravity data tied against an absolute base station in Southampton and a relative station established on the quayside in Port of Spain during JC102. The swath bathymetry data were calibrated with a sound velocity dip undertaken at the lateral centre of the ocean-bottom seismograph grid; the same location as sampled during JC102. Despite delays to the start of the cruise and bad weather crossing the Bay of Biscay, all seabed instruments were successfully recovered. On average, each ocean-bottom seismograph recorded data continuously for 198 days, with initial quality control review revealing numerous local events each hour through the deployment window, together with a number of global teleseismic events recorded throughout the deployment window.

1. Background and scientific objectives

1.1 Background

Since the discovery of domal corrugated surfaces at slow-spreading mid-ocean ridges (Cann et al., 1997), our understanding of how seafloor spreading works has radically changed. These domal surfaces, termed oceanic core complexes, were believed to be the unroofed plutonic and partially serpentinitized mantle footwalls of large-offset normal 'detachment' faults; structures apparently responsible for accommodating much of the plate separation. These detachment faults are believed to cross-cut the entire crust, exhuming in their footwalls first a crustal section (typically a non-corrugated blocky massif) and then, in the domal oceanic core complex (OCC - Fig. 1), mantle rocks intruded by plutonic gabbros (Tucholke and Lin, 1994; Cann et al., 1997; Tucholke et al., 1998). The OCC is commonly striated and corrugated in the spreading direction (Fig. 1) and interpreted to be a slip surface, exhumed from beneath median valley basalts.

Many aspects of this newly recognised mode of seafloor spreading remain unproven or controversial. For example, although it is likely that the corrugated upper surfaces of OCCs represent the exposure of steeply dipping detachments rooting at depth beneath the median valley, the link has not been clearly proven, though it is supported to some extent by palaeomagnetic studies (Morris et al., 2009; MacLeod et al., 2011) that show significant footwall rotation.

The only in situ evidence to date is based on P-wave travel-time tomographic inversion of two 2D wide-angle seismic profiles and passive micro-seismicity monitoring near the TAG hydrothermal field (Fig. 2 - deMartin et al., 2007). There, a steeply dipping band of hypocentres is inferred to mark a fault that flattens abruptly upwards to follow an unconnected, shallower, gently-dipping boundary between two velocity anomalies, one of which, reflecting a region of higher relative velocity, is located in the footwall. However, the TAG data does not directly image the detachment rollover, does not prove the continuity between steep and shallow zones, and does not show the lateral extent of the detachment.

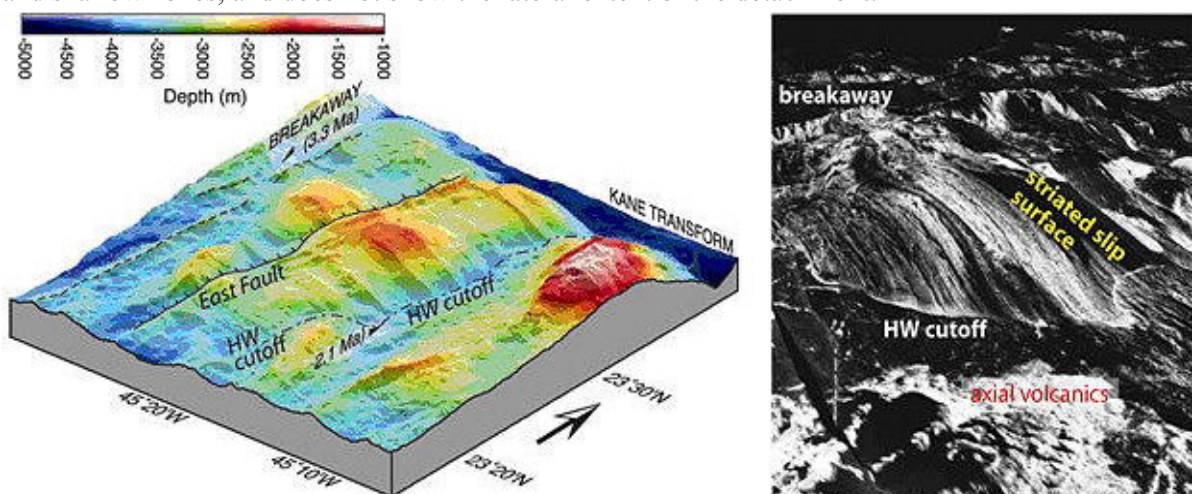


Figure 1: Perspective views of two typical Atlantic OCCs: Kane B (left) and 1320 (right). Both show corrugated/striated exhumed slip surfaces, the breakaway and hanging-wall cut-offs, but whereas Kane B has been rafted off-axis and so is no longer actively being exhumed, 1320 is still being pulled out from beneath a gap (dark area bottom right) in a zone of axial volcanics (rough, light tones).

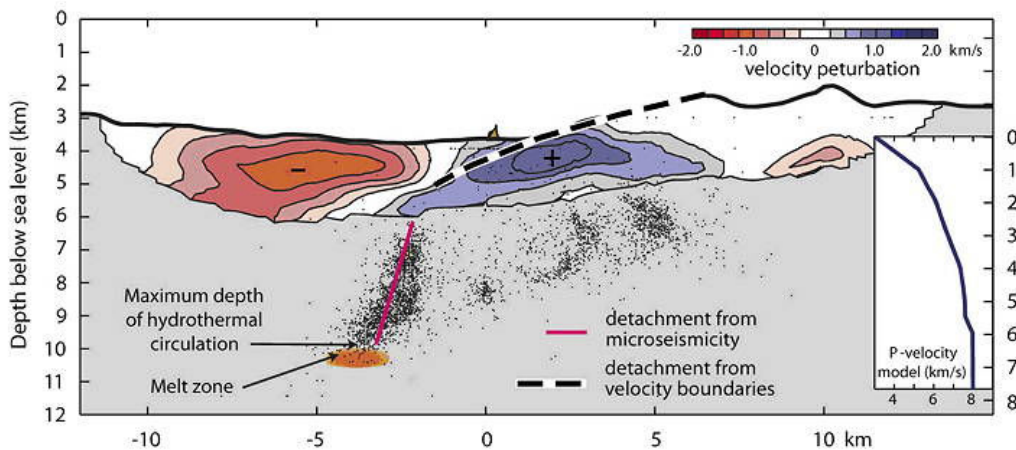


Figure 2: Section through the TAG area (deMartin et al., 2007), showing a possible detachment partly defined as a velocity boundary and partly as a zone of dipping micro-seismicity.

Escartin et al. (2008) and Reston & Ranero (2011) see oceanic detachment faults as essentially continuous, long-lasting features active on a segment scale (Fig. 3). Here, OCCs are simply places where a mega-detachment breaks surface, being covered in the intervening regions by thin-skinned rider blocks of volcanic seafloor. If so, as much as 50% of Mid-Atlantic Ridge (MAR) crust may be the result of asymmetric detachment faulting; it has even been suggested that mantle-derived material may dominate huge swathes of Atlantic ocean floor, potentially forming 20-25% of all seafloor produced at spreading rates <40mm/yr (Cannat et al., 2010).

Alternatively, MacLeod et al. (2009) see OCCs as spatially restricted, ephemeral features that are switched on and off by variations in local magma supply (Fig. 4). In this model OCC detachments are ordinary valley wall faults on which slip continues as a result of the progressive waning of magma supply to below half that needed to generate a continuous igneous crustal layer. Strain localisation would result in progressively more asymmetric plate separation, until more than half is partitioned onto the detachment itself. As this occurs, the detachment migrates towards and across the axial valley, such that renewed magmatism is intruded into the detachment footwall and ultimately overwhelms it. Spreading becomes strongly asymmetric between a localised OCC and its immediate conjugate, but not across the whole of a spreading segment. The lateral change in spreading asymmetry and the limited dimensions of the detachment fault in this model require spatially restricted transfer zones (dominated by magmatism and ductile shear at depth and faulting near surface) to accommodate the along-strike variations in strain distribution.

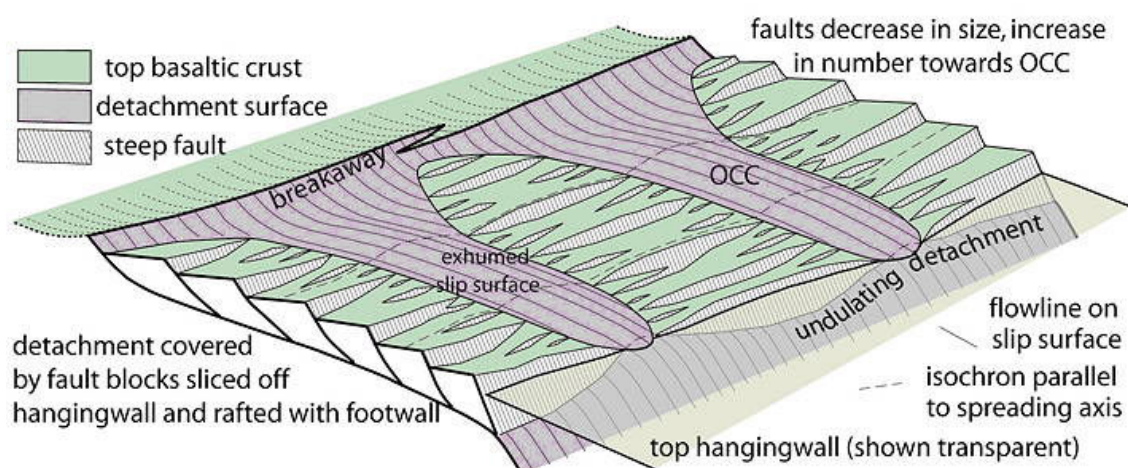


Figure 3: Perspective view of the segment scale detachment model: the detachment continues laterally beneath small fault blocks between adjacent OCCs, which represent the places where the detachment breaks the surface. In the alternative model, adjacent OCCs are unconnected.

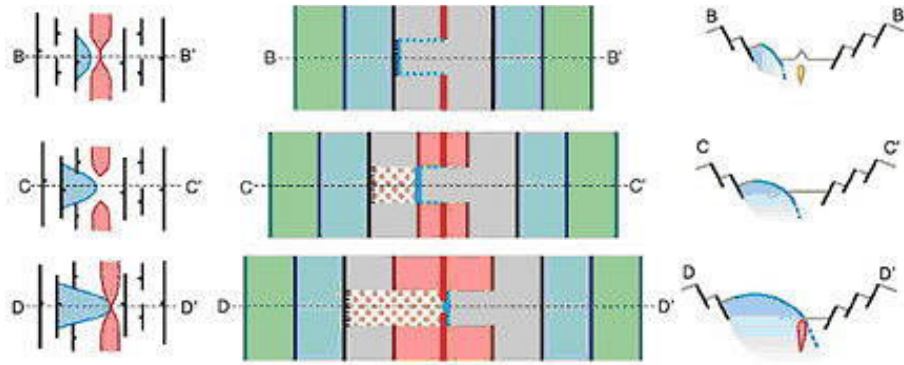


Figure 4: MacLeod et al. (2009) model for OCC formation: strain weakening concentrates deformation onto a single fault which accommodates more than half the total spreading, and so migrates toward and over the spreading axis, to be cut by renewed magmatism. Left: structural map; Middle: magnetic lineations; Right: schematic sections.

There are, therefore, two conflicting hypotheses:

1) detachments continue laterally between OCCs which are linked (Reston and Ranero, 2011)

and

2) detachments are temporally and spatially restricted and not linked (MacLeod et al., 2009).

The two conflicting hypotheses (**1. linked vs. 2. restricted**) make testable predictions:

- 1a:** Detachments continue in the sub-surface between OCCs and so control divergence at a whole spreading segment for extensive periods of time;
- 1b:** Asymmetric spreading affects the whole segment, not just OCCs and their conjugates;
- 1c:** By controlling spreading of an entire segment, the detachment drives mantle upwelling and location of the spreading axis.
- 2a:** Detachments are restricted to individual OCCs and are thus localised in time and space;
- 2b:** OCCs produce spatially restricted spreading asymmetry that does not extend segment-wide; strain is transferred laterally by magma injection and brittle deformation;
- 2c:** Gabbros are only incorporated into the footwall late as it migrates across the median valley.

We can test the above hypotheses by determining:

- (a)** the sub-surface geometry of detachment faults at active OCCs, and how this changes in extent both along- and across-strike beneath adjoining volcanic-dominated seafloor;
- (b)** the local degree of asymmetry of plate separation adjacent to an OCC compared to the adjoining volcanic seafloor; and
- (c)** the amount and distribution of melt delivered to both hanging wall and footwall at an active OCC in comparison to that in the adjoining volcanic seafloor region.

The required data from an actively forming OCC do not exist, and we will collect them during three cruises to the MAR between $\sim 13^{\circ}15'$ and $13^{\circ}35'N$. This report describes the second of these cruises – the passive micro-seismicity ocean-bottom seismograph recovery.

1.2 The study location - $13^{\circ}N$

An extensive region of OCCs exists at $13^{\circ}N$ on the MAR, and includes two located at $13^{\circ}20'N$ (henceforth known as 1320) and $13^{\circ}30'N$ (1330) that are actively developing, making this region the ideal target for this study. These OCCs have already been surveyed with shipboard multi-beam swath bathymetry (Smith et al., 2008), imaged with TOBI near-bottom side-scan and sampled with dredges and a seabed rock-drill (Searle et al., 2007; MacLeod et al., 2009; Mallows, 2011; Mallows and Searle, 2012).

Apart from the wealth of existing data, 13°N is the ideal location for this study because:

- unlike other fully-developed OCCs both 1320 and 1330 can be traced directly to the spreading axis, implying that both are currently active;
- the typical, high reflectivity, untectonised hummocky terrain of the MAR neovolcanic zone (NVZ) is absent opposite 1320 and 1330 (Fig. 1), and is replaced by lower reflectivity terrain (suggesting older volcanics with several metres of sediment cover), often displaying small-scale faulting. This, and a concomitant increase in tectonic strain, is interpreted as evidence that the melt supply is reduced near the regions of active detachment faulting (MacLeod et al., 2009);
- the NVZs north and south of 1320 taper toward it, suggesting they are propagating towards this magmatic gap and may ultimately “switch off” the detachment faulting, as appears to have been the case for the off-axis OCC at 13°48’N; and finally and crucially
- the presence of two active OCCs that developed at similar times and which remain active implies either that the controlling detachment continues under the intervening basin or that the basin is a zone of magmatic soft linkage between two spatially limited detachment systems.

1.3 Scientific objectives

The primary objectives of this project are to test the different and contrasting hypotheses for the spatial and temporal evolution of OCCs. From all three cruises acquiring the necessary geophysical data, we will determine:

- 1) the geometry of the detachments that have unroofed the 1320 and 1330 OCCs, (i) through direct imaging of the detachment surface with multichannel seismic (MCS) reflection data, and (ii) by imaging with ocean-bottom seismograph (OBS) wide-angle (WA) data any intra-crustal layering (refracting interfaces) and regions of mantle-derived material and melt accumulation (relative velocity anomalies), in both cases from the seabed down to sub-Moho, and (iii) from the distribution of seismicity down to the base of the brittle lithosphere, probably 7-8 km sub-seafloor (testing **Hypotheses 1a, 1c, 2a, 2c**);
- 2) the lateral extent of the 1320 and 1330 detachments, through a combination of direct (MCS reflection) and indirect (WA velocity structure) imaging, and distribution of seismicity (testing **Hypotheses 1a, 2a**);
- 3) the detailed spreading history and thus any along-segment variation in the asymmetry of spreading, through high-resolution Autosub magnetic imaging (testing **Hypotheses 1b, 2b**);
- 4) the detailed internal structure of the footwall of the detachment, both at the spreading axis and at an OCC, through a combined approach of 3D seismic velocity tomography and magnetic field inversion (testing **Hypothesis 1c, 2c**); and
- 5) we will also collect high-resolution bathymetry data simultaneously with magnetic field measurements on Autosub 6000, which will aid structural interpretation of, for example, OCC domes, the inferred exhumed Moho and tectonic linkages. We will also use Autosub to identify locations of fluid outflow (fault scarps, hydrothermal systems and exposures on the corrugated surface – Connelly et al., 2011) and future sampling sites from the nephelometer, CTD, Eh and ADCP data collected contemporaneously with the high resolution bathymetry and magnetic data. These data will also constrain the precise geometry and extent of the hydrothermal discharge inferred at the toe of 1320 from the massive sulphides recovered there on JC007 (Searle et al., 2007), and thus inform our understanding of the thermal structure of the OCC and likely implications for controls on the larger-scale rheology.

Leg 2, JC109, aims to recover the OBS deployed during Leg 1 (JC102) for a 6-month duration local micro-seismicity survey. Finally, Leg 3 aims to complete active-source MCS and WA seismic acquisition and Autosub 6000 surveying.

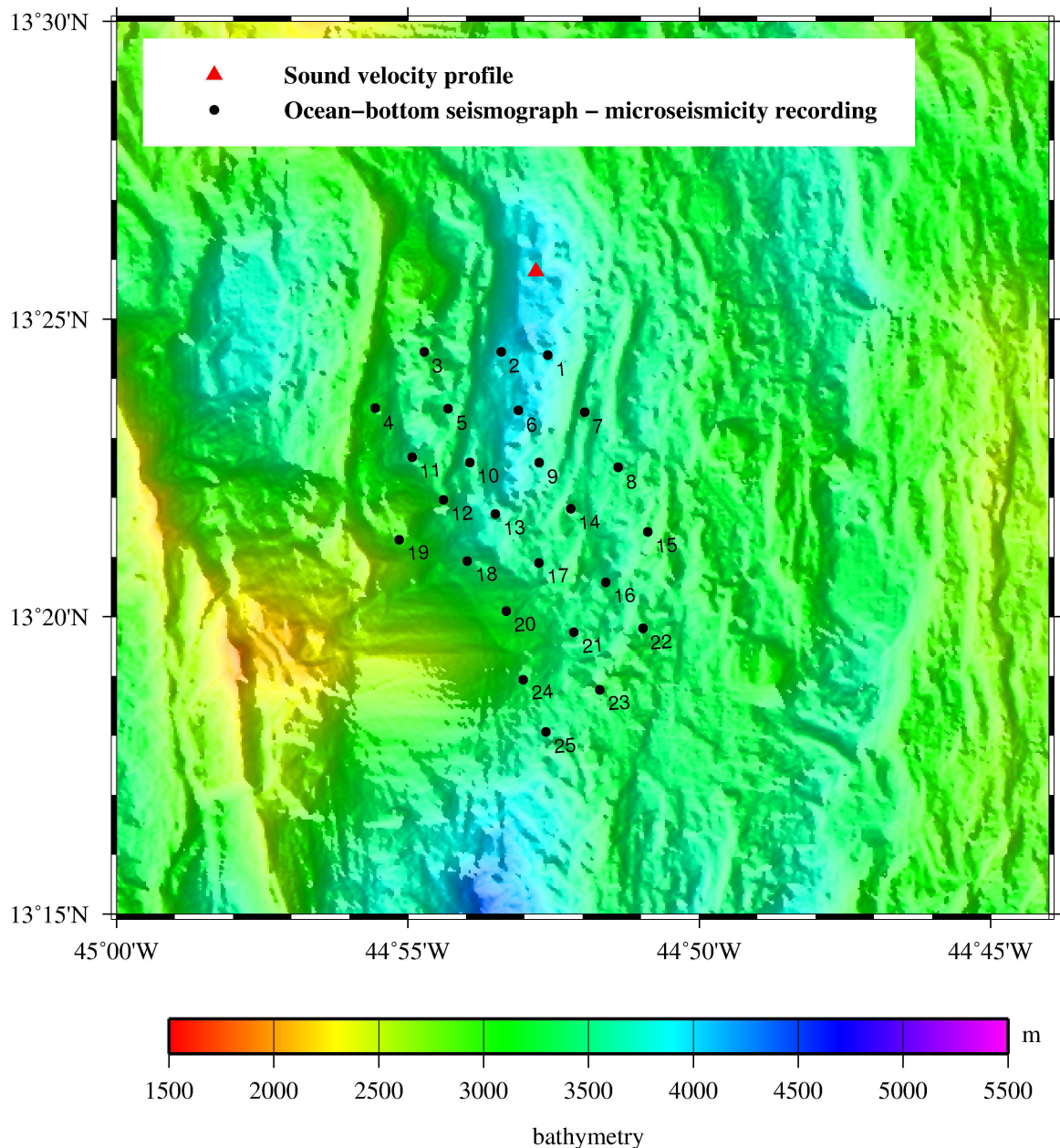


Figure 5: JC102 OBS deployment locations for passive micro-seismicity recording. All OBS were equipped with a three-component 4.5 Hz, gimbaled geophone pack. OBSs 1, 3, 5, 7, 12, 14, 15, 17, 20 & 23 were equipped with differential pressure gauges. The remaining OBSs were equipped with a hydrophone.

For the JC102 deployment we followed the approach adopted by Project Partner Sohn at the TAG area (deMartin et al. 2007). We deployed 25 OBS in a tight network centred on the most ridge-ward limit of the 1320 OCC and extending to the north (Fig. 5 and Table 1 for OBS locations). The deployment locations were concentrated over the northern half of the 1320 detachment, close to its hanging wall cut-off (where the detachment passes beneath the seafloor) and continue to the north approximately halfway towards the 1330 OCC, to map out the postulated lateral continuation of the master detachment between OCCs. Given the known amount of teleseismic activity from the study area, we estimated that ~50 locatable earthquakes would take place every day. By recording for 6 months, we expected to record ~9000 earthquakes and we expect these to be representative of the active faulting in the region.

2. Cruise preparation and mobilisation

2.1 Scientific plan

The port call at the start of the cruise was Southampton (UK), which was ~14 days from the work area at a transit speed of 10 kn. The OBS recovery would take ~3 days including a sound velocity profile and acoustic release system tests, followed by 3.5 days of swath bathymetry surveying. The end of cruise port call was Port of Spain (Trinidad), about 4.5 days transit from the work area. The entire cruise was, thus, 25 days port-to-port. The way points for the cruise can be found in Table 1.

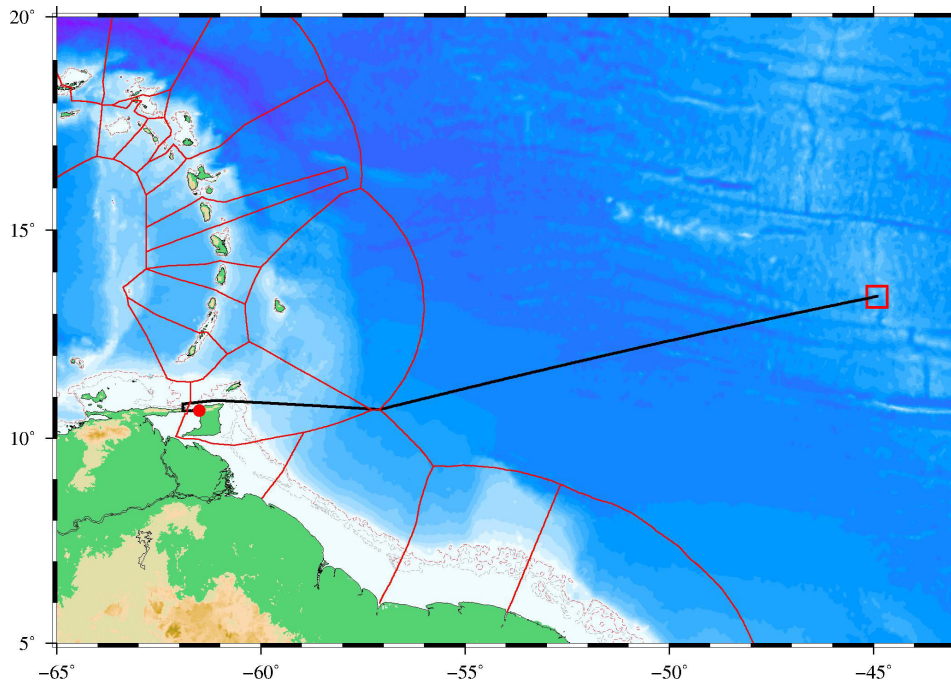


Figure 6: Work area plotted relative to the EEZs of the Caribbean region, together with the proposed transit track to Port of Spain.

2.2 Territorial waters and diplomatic clearances

The work area for this cruise lies entirely in international waters as shown in Fig. 6. We also planned to run the gravimeter and swath bathymetry acquisition all the way from and to the ports of call to enable start and end of cruise base station ties. Consequently, diplomatic clearance from Trinidad and Tobago was required. Despite completion of the paperwork to enable the clearance application to be submitted at least six months prior to arrival at the 200 nm limit of Trinidad and Tobago, and despite chasing for clearance in the days preceding arrival, once a response was received clearance was initially declined for reasons that currently remain unclear. With no permission to enter Trinidad and Tobago waters the vessel was instructed to remain at the 200 nm limit on arrival until the Foreign and Commonwealth Office could resolve the matter. With the assistance of the Office of the High Commissioner for Trinidad and Tobago, clearance was eventually received ~24 hours after reaching the 200 nm limit.

2.3 Mobilisation

All equipment containers were loaded onto the vessel in Southampton. Mobilisation commenced on the 9th October with a sailing date of the 08:00 (local = GMT+1) on the 11th October. The JC109-related port call activities solely related to the unloading and secure stowage of the ocean-bottom seismograph (OBS) peripheral equipment, including the data processing server, and undertaking the absolute gravity base tie at the National Oceanography Centre station adjacent to the vessel.

2.4 Delays to sailing

Prior to JC109, the RRS Cook had a scheduled period of refit works in Santander followed by a short set of trials to, amongst other things, test and calibrate the newly fitted swath transducers. Part of these refit works related to a set of fittings on each of the vessels lifeboats which also required inspection by the Maritime and Coastguard Agency (MCA). The refit works were found to be non-compliant and replacement parts required re-fabrication in Southampton and subsequent inspection by the MCA. Despite sailing being scheduled for 08:00 on Saturday 11th October, these works were not completed until Monday 13th October.

A further delay to sailing was due to documentation submitted for customs clearance for export licence-controlled equipment loaded onto the vessel in preparation for JC114, being deemed unacceptable by HM Revenue and Customs, resulting in a new licence having to be sought and the associated documentation being amended accordingly. The vessel eventually sailed at 18:50 (local = GMT+1) on Tuesday 14th October, a delay of ~3.5 days. To try and make up for this delay, permission to run three engines was granted and five days of addition fuel bunkered. Once a region of bad weather in the Bay of Biscay had been traversed, use of three engines enabled a transit speed of 15 kn, for five days of the subsequent transit.

3. Work conducted and data collected

A track chart for the entire cruise is shown in Fig. 7, a blow-up of the work area only is shown in Fig. 8. The data acquisition comprised: i) ocean-bottom seismograph recoveries; ii) sound velocity profiling; iii) gravity; and iv) swath bathymetry surveying. Each of these data types and the equipment used will be described in the following sections.

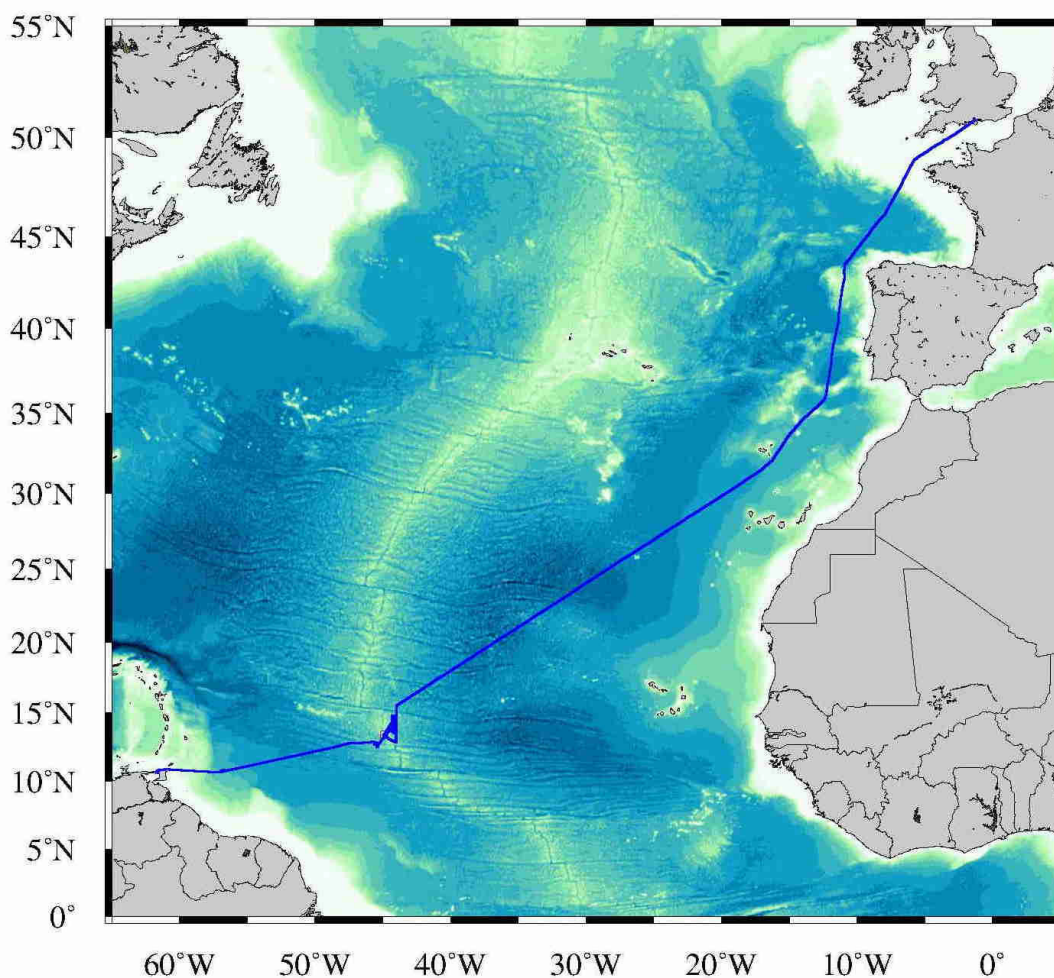


Figure 7: Track chart for JC109.

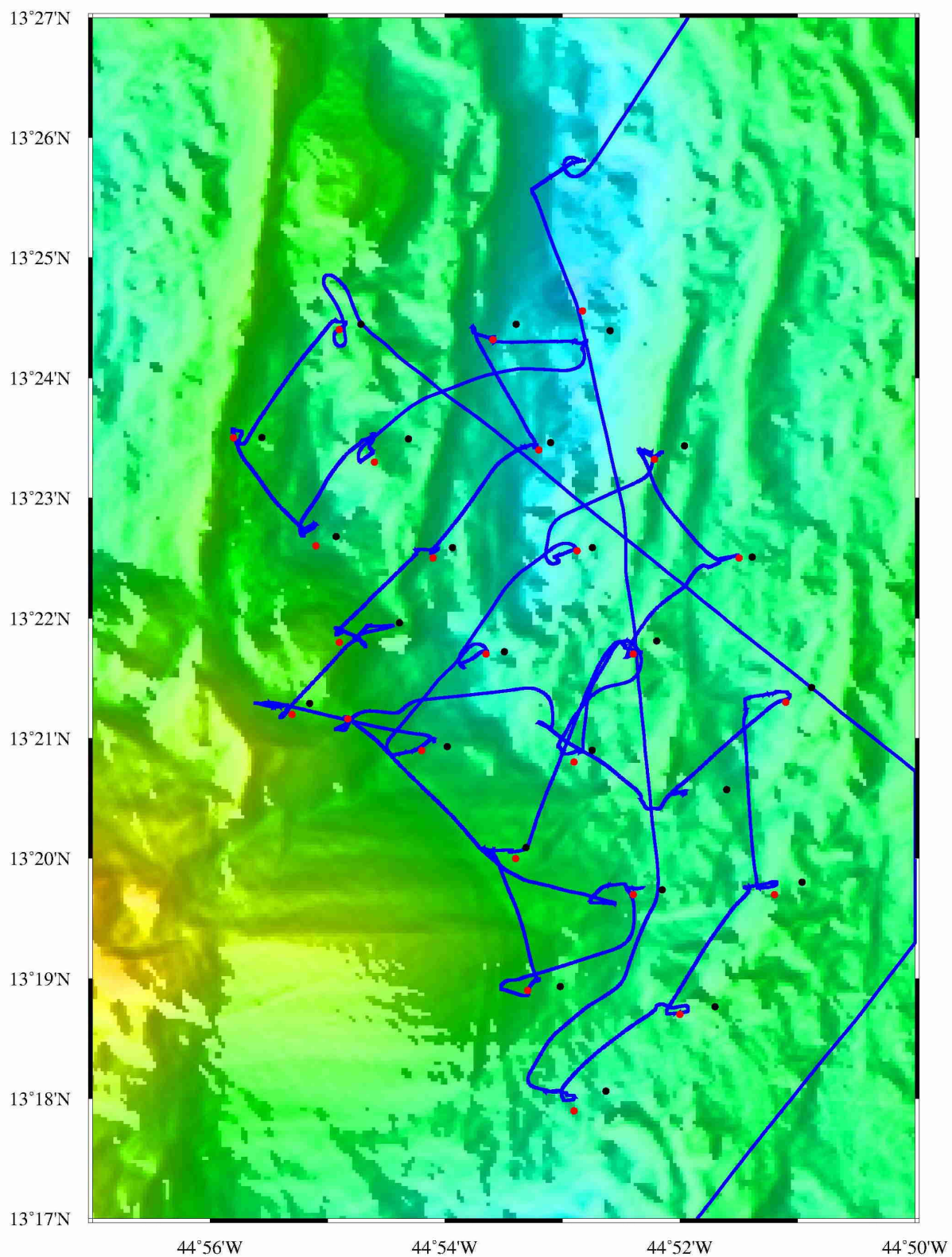


Figure 9: Ocean-bottom seismograph recoveries. Red dots show recovery positions relative to deployment locations (black dots), while the blue line shows the vessel track. In general, a strong ~1 kn current took each instrument to the west of its deployment location.

The maximum duration of recording of any of the OBSs was 198 days and 14 hrs – from Julian day 103 (13th April, 2014) to 301 (28th October, 2014), with the raw data converted to the standard miniSEED format (<http://ds.iris.edu/ds/nodes/dmc/data/formats/>) used for passive seismic recording. Two example data sections are included below as Figs 10 (global teleseismic event) and 11 (local micro-seismicity).

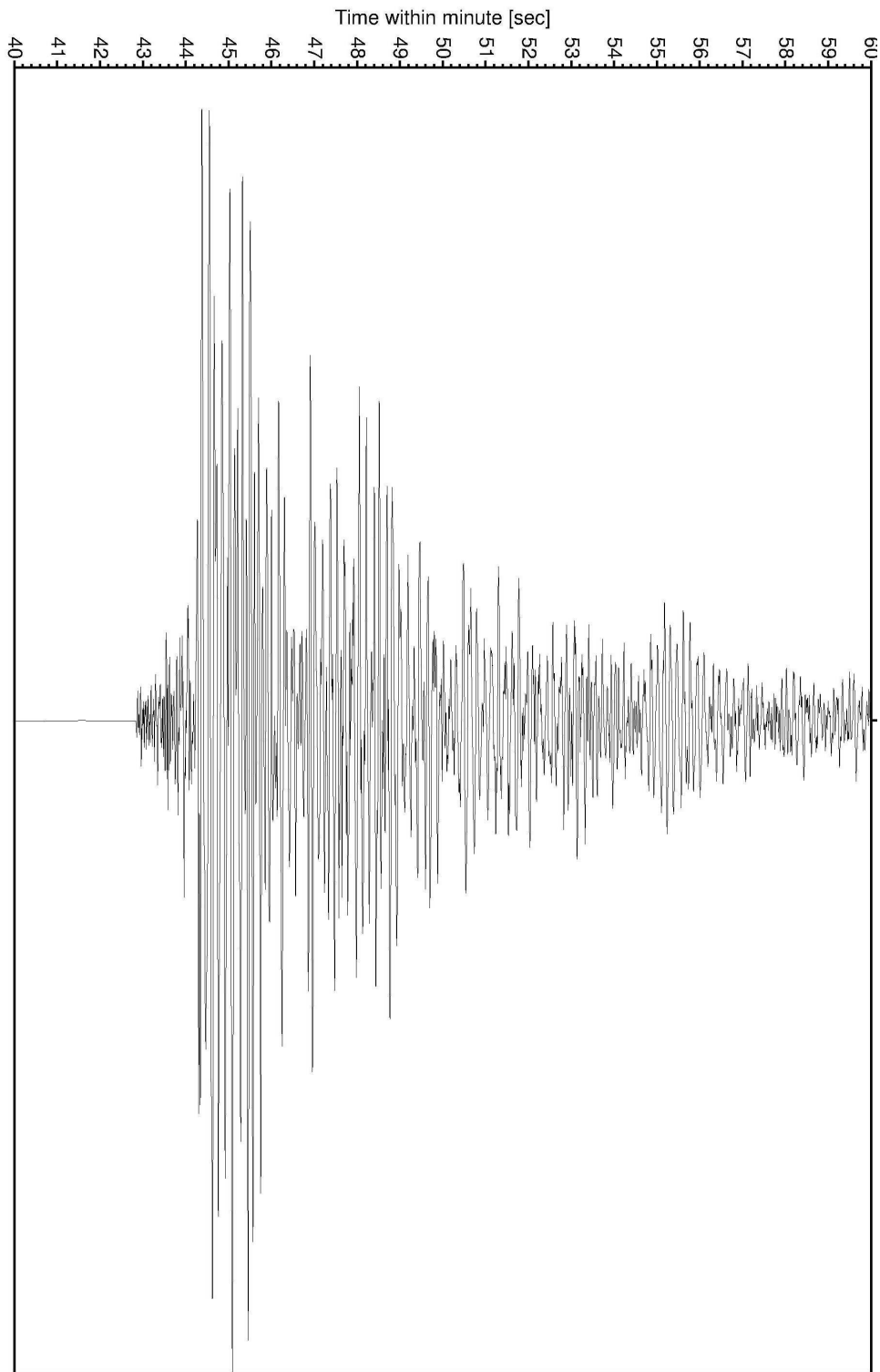


Figure 10: Vertical geophone recording of the 23rd August 2014 Chile earthquake – M_b 6.4 located at 32.64°S 71.34°W.

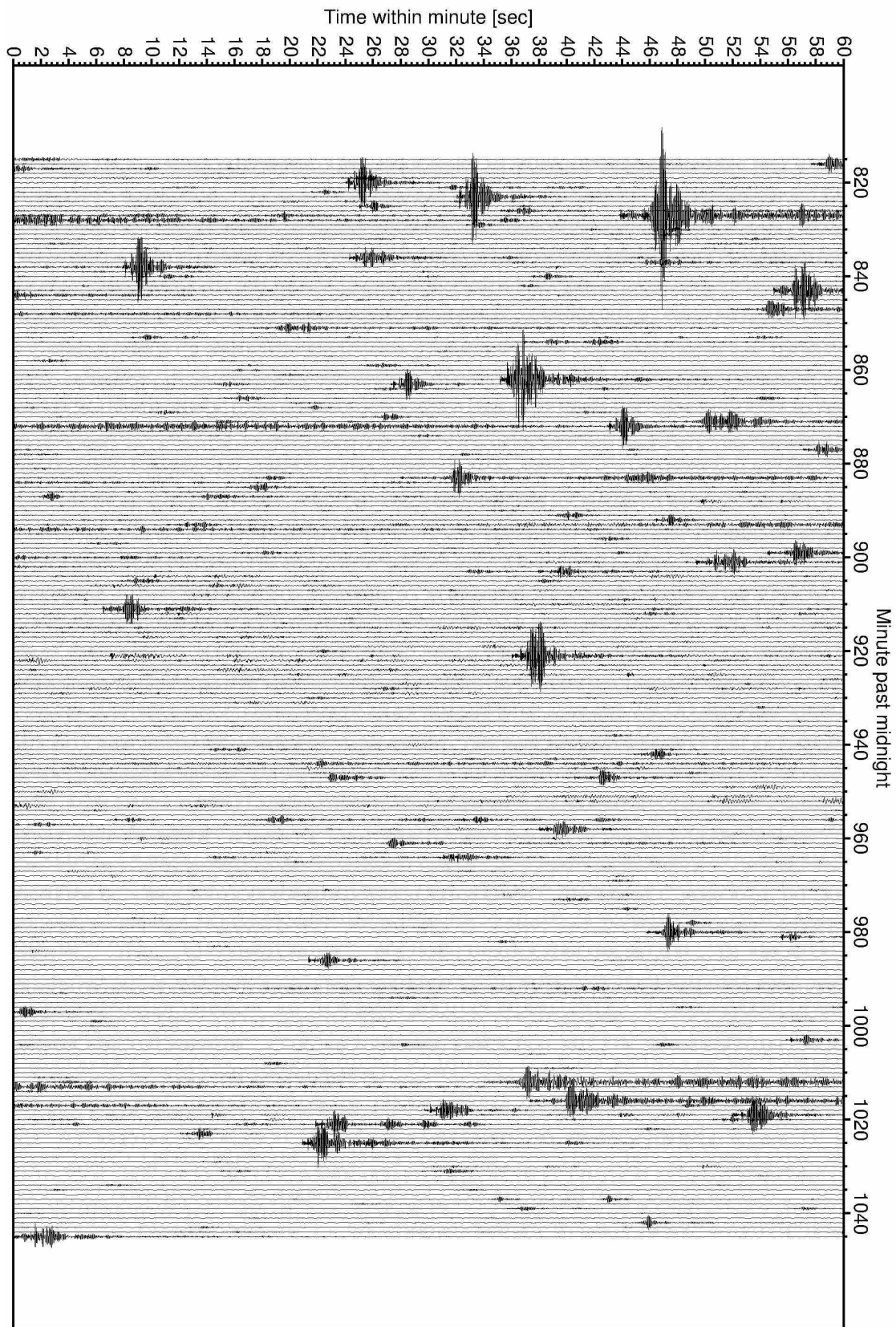


Figure 11: Local seismicity in the study area for the period 13:28 to 17:24 GMT on 23rd June (day 174). The data shown are from the vertical geophone and is unfiltered.

3.2 Sound velocity profiling

A sound velocity profile was conducted in the north of the work area (see Table 3 for deployment location) using two Valeport Midas sound velocity probes simultaneously. This profile was used to calibrate the EM120 swath bathymetry system. The resulting profile is shown in Fig. 12, plotted relative to the sound velocity profile acquired in the same location during JC102 for comparison.

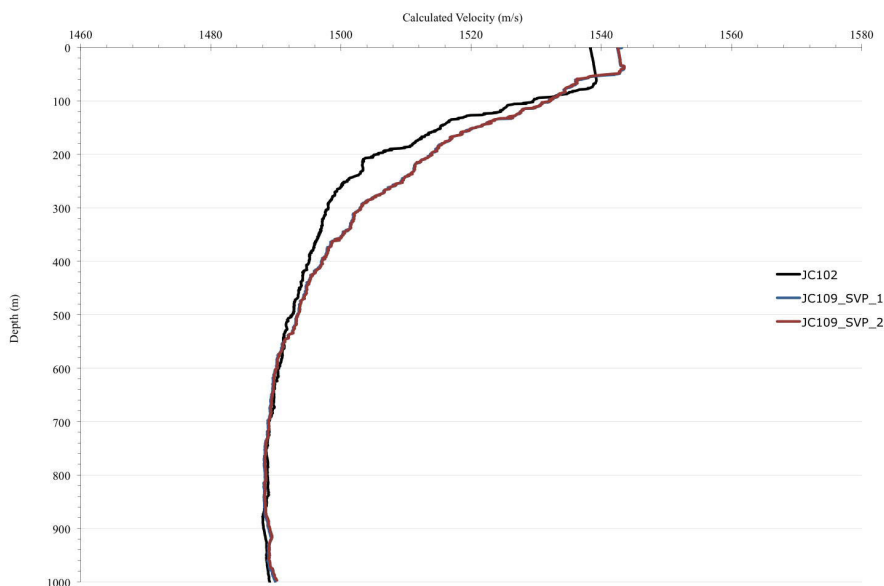


Figure 12: Sound velocity profile for JC109 (red, blue) plotted against the JC102 profile (black) from the same location.

3.3 Gravity

Gravity data were acquired using a Lacoste-Romberg air-sea gravimeter (S-40) mounted on a gyro-stabilised platform. The gravimeter was “tied-in” to an absolute base station at the NOC, Southampton, prior to departure and to a relative gravity base station established on the quay in Port of Spain during JC102. The original Port of Spain absolute gravity base station was located at the airport, and is now inaccessible. An example processed (for QC purposes only) data profile from the cruise is shown in Fig. 13. The gravity base station details are summarised in Table 4. The only data loss experienced during JC109 occurred when a mains power breaker tripped and terminated logging of all underway systems. Fortunately, the gravimeter’s UPS maintained the embedded sensor heater until the breaker could be reset and logging restored.

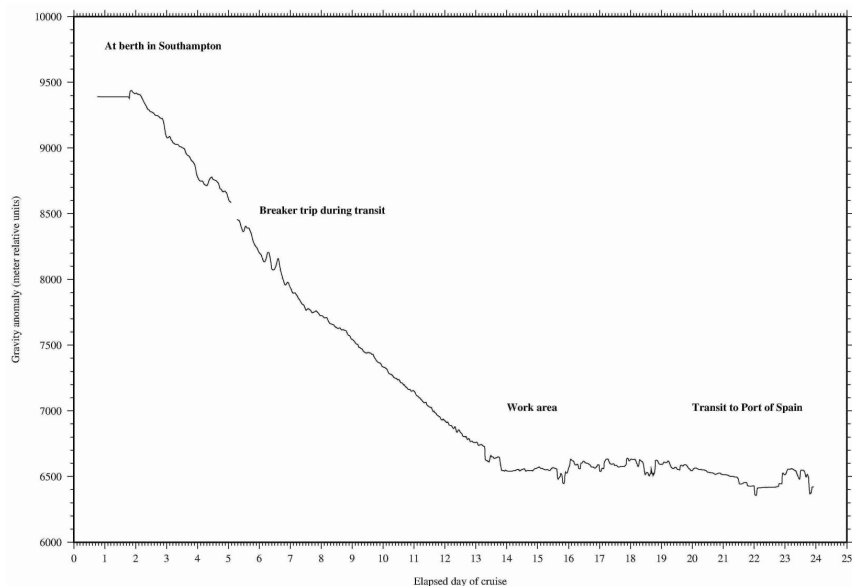


Figure 13: Relative gravity profile for JC109.

3.4 Swath bathymetry data

The RRS James Cook is fitted with a Kongsberg Simrad EM120 multi-beam deep ocean echo sounder. Data acquisition is based on successive transmit-receive cycles with the beam width optimised to match the sea conditions. Seabed depth and reflectivity are recorded against GMT time and GPS location. Swath bathymetry data were acquired port-to-port. All swath bathymetry data acquired from the work area to the Port of Spain port call is shown in Fig. 14, and that for JC102 and JC109 combined is shown in Fig. 15. The transit route to Port of Spain was chosen to broaden the swath coverage acquired during JC102. The combined data set for the work area alone is shown in Fig. 16. It proved possible to acquire clean, good quality data at 15 kn (level keel ballasted) into the sea during this cruise, with a dramatic improvement in data quality observed at speeds above 12.5 kn. At all lower speeds, with the vessel on a heading into the sea, data quality proved poor. Fig. 16 shows a comparison between ship's speed, centre beam "drop-out", pitch and heave for an easterly heading into the prevailing sea and wind speed at and above 20 kn. Not only does the vessel pitch and heave reduce above 12.5 kn, but centre beam drop-outs are significantly reduced.

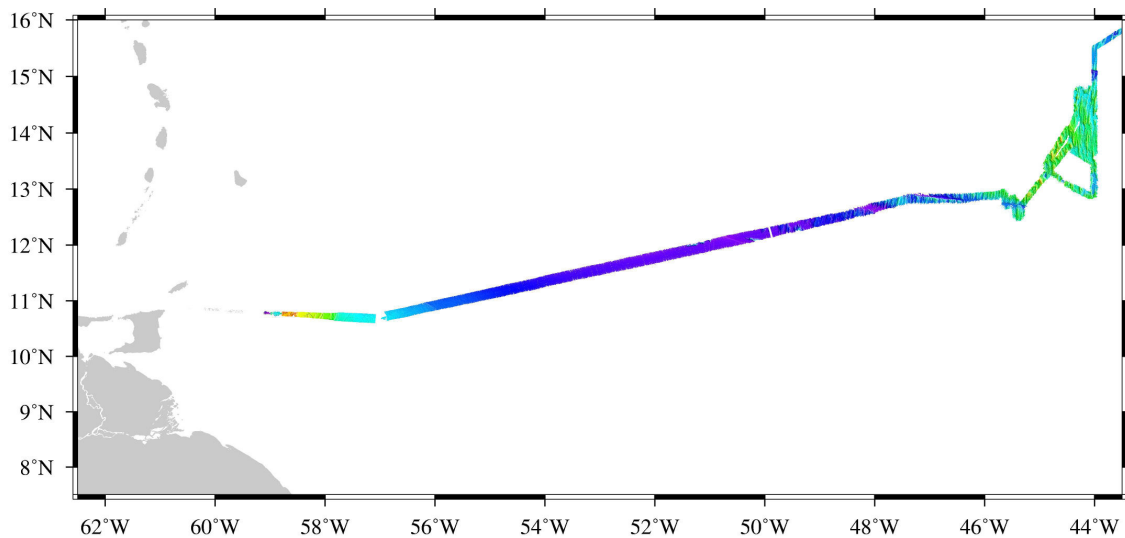


Figure 13: Swath bathymetry data for the work area to the Port of Spain port call.

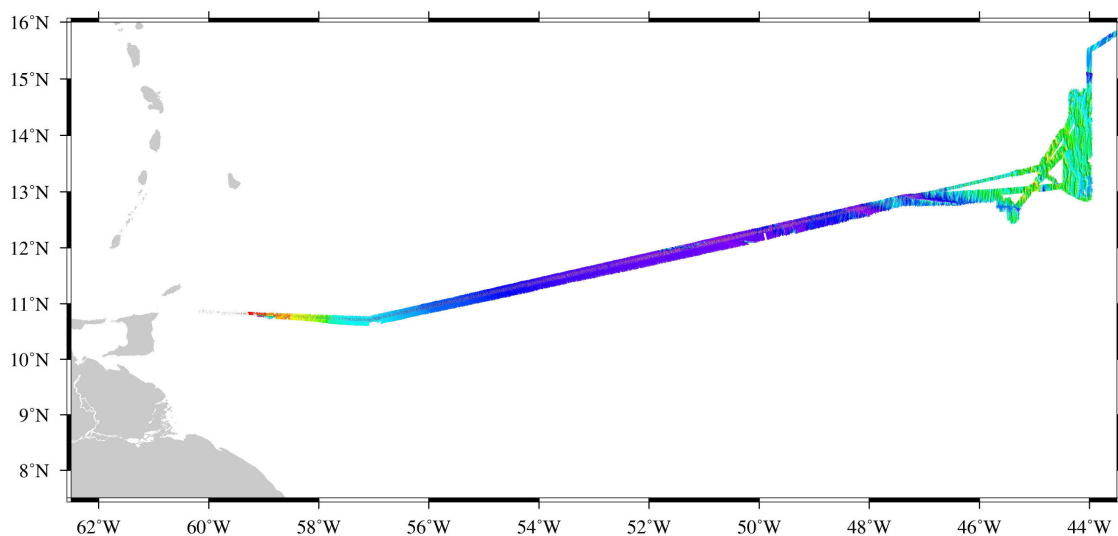


Figure 14: Swath bathymetry data for the work area to Port of Spain for JC102 and JC109 combined.

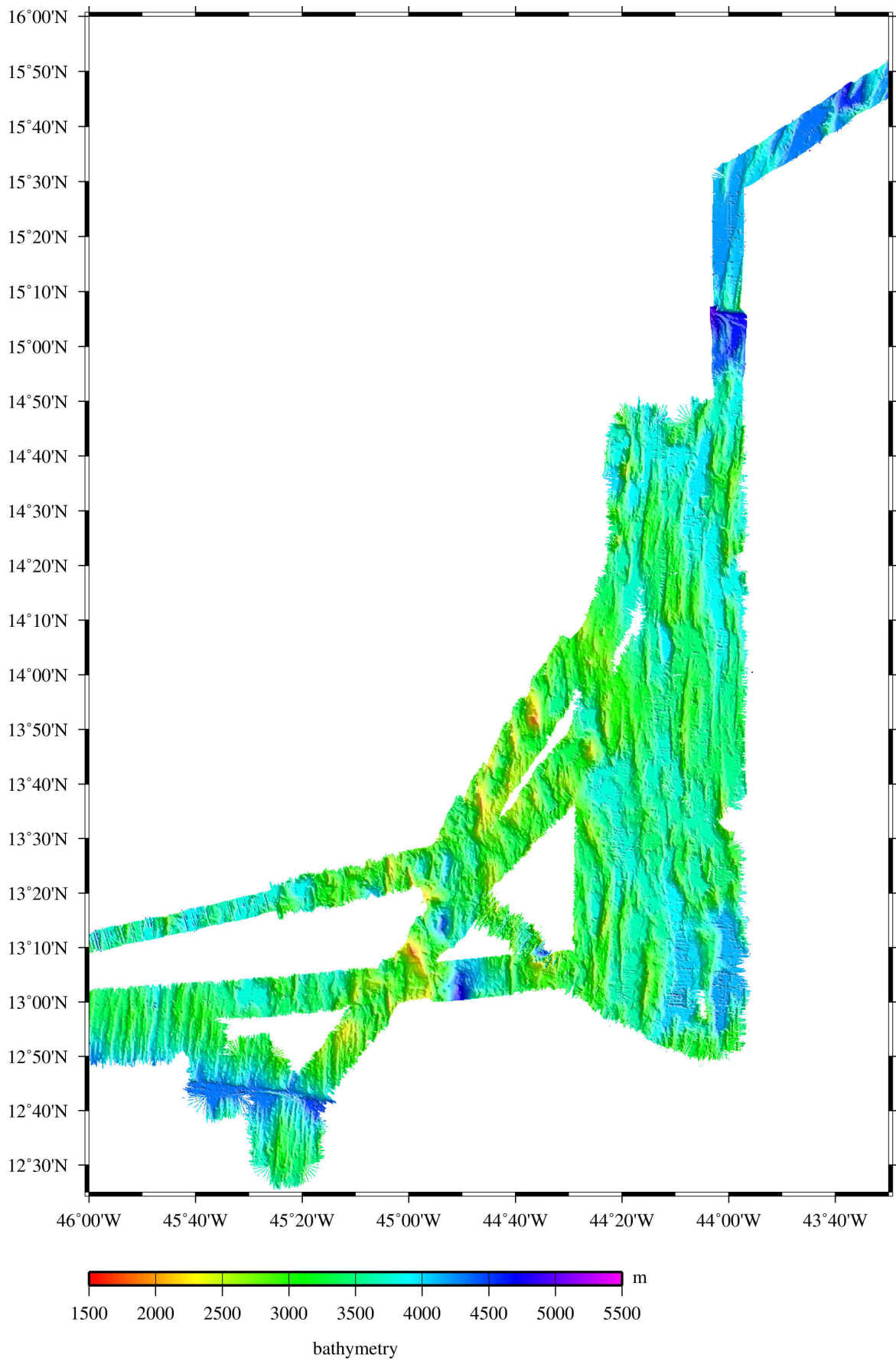


Figure 15: Swath bathymetry data for work area for JC102 and JC109 combined.

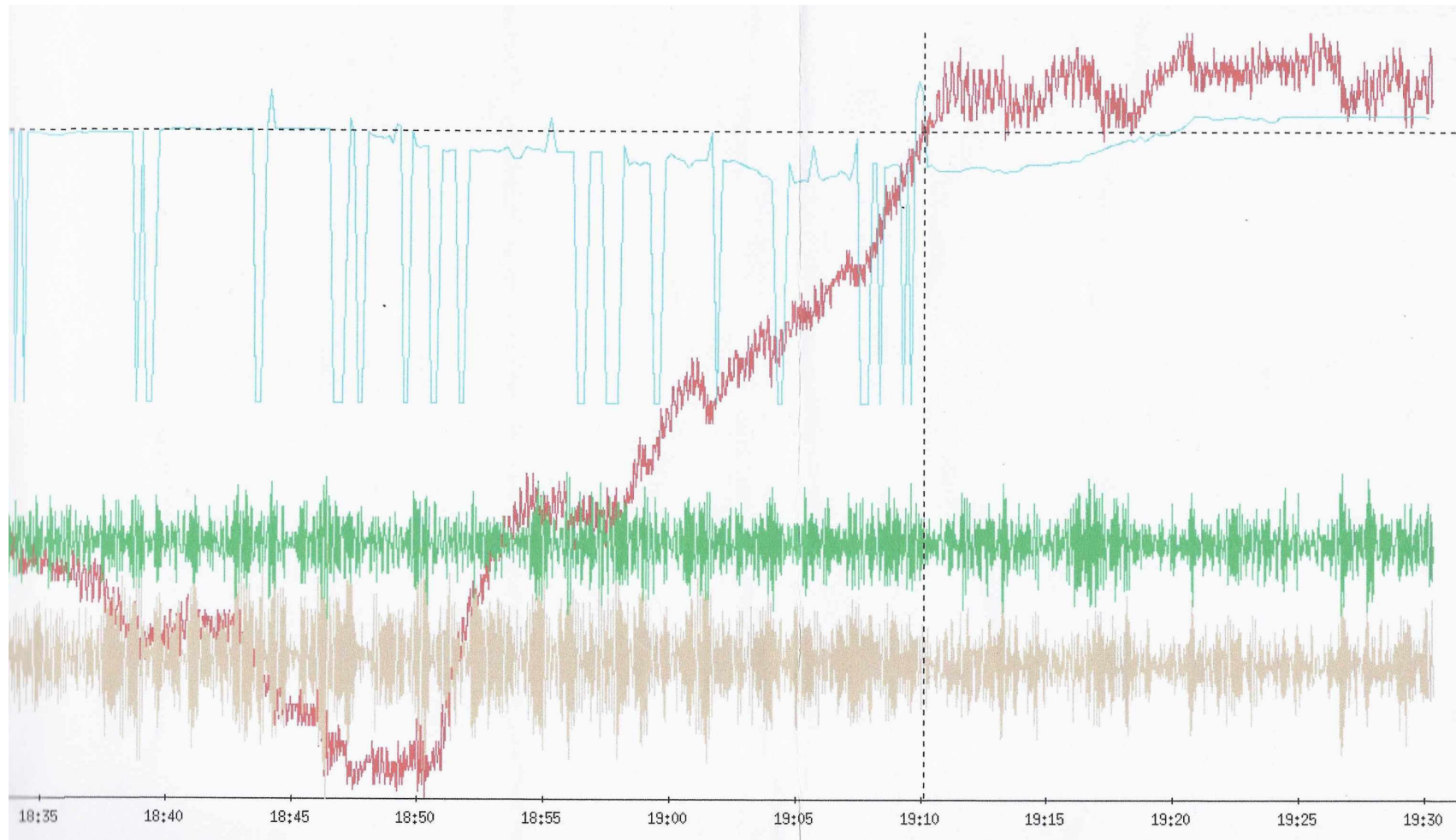


Figure 16: Comparison between ship's speed (red), centre beam "drop-out" (blue), pitch (brown) and heave (green) against time. Horizontal dashed line indicates a speed of 12.5 kn. Centre beam "drop-outs" reduce significantly above this speed, as does vessel pitch and heave. At slower speeds into the prevailing sea, drop-outs were significant and the swath data quality poor.

4. Cruise narrative

The duration of the cruise was 22 days and 2 hours. Of this, ~16.5 days were spent on passage to and from port calls to the work area, leaving a total of ~5.5 days in the work area. Of the latter ~2.25 days were spent recovering OBSs and ~3.25 days for swath bathymetry acquisition. A summary of the events that took place appears below. All times are in GMT (UTC), all way points are listed in Table 1, and cruise track charts are plotted in Figs 7 and 8.

Julian Day	Date	Time (GMT)	Activity
284	Saturday 11 th October	All day	Berthed pending rectification works on lifeboats and HMRC clearance.
285	Sunday 12 th October	All day	Berthed pending rectification works on lifeboats and HMRC clearance.
286	Monday 13 th October	All day	Berthed pending rectification works on lifeboats and HMRC clearance.
287	Tuesday 14 th October	14:00 17:50	Berthed pending HMRC clearance. Bunkers of additional fuel. Departure from Southampton.
288	Wednesday 15 th October	All day	On passage.
289	Thursday 16 th October	All day	On passage.
290	Friday 17 th October	All day	On passage.
291	Saturday 18 th October	All day	On passage.
292	Sunday 19 th October	All day	On passage.
293	Monday 20 th October	All day	On passage.
294	Tuesday 21 st October	All day	On passage.
295	Wednesday 22 nd October	All day	On passage.
296	Thursday 23 rd October	All day	On passage.
297	Friday 24 th October	All day	On passage.
298	Saturday 25 th October	All day	On passage.
299	Sunday 26 th October	04:05 08:07 12:44 16:48 18:34 18:36 19:33 20:56	Arrival at WP T_1. Arrival at WP T_2. Arrival at WP T_3. Arrival at WP ACOUSTIC, commencing acoustic release, SVP and USBL beacon tests. Acoustic tests complete. Commence passage to first OBS recovery position. OBS_25 released. OBS_25 recovered.

		22:12 23:33	OBS_23 recovered. OBS_22 recovered.
300	Monday 27 th October	01:30 06:32 08:24 09:50 11:15 12:42 14:10 15:24 16:52 18:04 19:50 21:10 22:39	OBS_15 recovered. OBS_16 recovered. OBS_21 recovered. OBS_24 recovered. OBS_20 recovered. OBS_17 recovered. OBS_14 recovered. OBS_08 recovered. OBS_07 recovered. OBS_09 recovered. OBS_13 recovered. OBS_18 recovered. OBS_19 recovered.
301	Tuesday 28 th October	00:40 02:08 03:36 05:14 06:48 08:13 09:31 10:41 11:50 12:12	OBS_12 recovered. OBS_10 recovered. OBS_06 recovered. OBS_02 recovered. OBS_01 recovered. OBS_05 recovered. OBS_11 recovered. OBS_04 recovered. OBS_03 recovered. OBS recovery complete. Swath surveying WPs T_3 to T_21.
302	Wednesday 29 th October	All day	Continuation of swath survey.
303	Thursday 30 th October	All day	Continuation of swath survey.
304	Friday 31 st October	08:02 16:25	Swath surveying WPs T_24 to T_27. End of science. Commence passage to Port of Spain.
305	Saturday 1 st November	00:00 06:16 11:16 12:00	On passage. Commencing stream of CTD wire for re-tensioning and re-spooling. Completed recovery of CTD wire. Recommence passage to Port of Spain.
306	Sunday 2 nd November	All day	On passage.
307	Monday 3 rd November	00:00 22:14	On passage. Arrival at 200nm limit of Trinidad and Tobago, hove to pending receipt of diplomatic clearance.
308	Tuesday 4 th November	00:00 22:42	Hove to pending diplomatic clearance. Diplomatic clearance received, recommencing passage to Port of Spain.
309	Wednesday 5 th November	00:00 19:00 20:00	On passage. Arrival at pilot station, Port of Spain. Alongside, Port of Spain. End of cruise.

5. Equipment performance

5.1 Ocean-bottom seismographs

Some of the recoveries undertaken during the hours of darkness proved quite challenging as either the flashing light or radio beacon (or both in one case), attached to each OBS as recovery aids, failed to turn on when at the surface. Instruments with failed flashing lights were, consequently, recovered using the traditional approach of ranging on their acoustic release transducer using a deck unit once the instrument had surfaced, and boxing to determine on which side of the vessel the instrument was located. Despite a strong westward current, and a number of faulty beacons, all 25 OBSs were recovered from the seabed during JC109. On inspection, the beacons were found to have failed pressure on-off switches, whose diaphragms had breached while deployed and allowed the ingress of water into the switch, with the light and radio units themselves remaining intact and otherwise functional. The instrument, whose flashing light was entangled in a strop on deployment with the entire instrument weight hanging from it (c. 200 kg), had been planned for recovery during daylight. On recovery the beacon was found to be bent and the diaphragm body parted from the main body of its switch. Of the 50 beacons deployed, 12 failed due to water ingress into the on-off switch, one pressure switch was damaged beyond-use by stropping, and one radio transmitted lost its antenna, which was suspected having appeared to have also been entangled in a strop on deployment, although it still broadcast on recovery.

All acoustic releases communicated on first command and all burnt their primary release burn wire on first command. Communication through a single element of the hull transducers negated the need to use a dunking transducer for recovery and enabled underway pinging to and releasing of each instrument on the seabed from the previous instrument site (variously between 1-2 nm) and ranging while each instrument ascended through the water column. The latter enabled calculation of rise rate and an accurate prediction of ETA at surface, allowing vessel positioning downwind within a few 100m of the predicted surfacing location. This ranging and vessel positioning (taking into account wind and current directions) made recovery onto deck rapid and eased the difficulty in locating at night instruments with failed flashing lights. On a positive note, the need to adopt the traditional ranging and boxing approach for some recoveries also acted as a good training opportunity for the less experienced members of the OBS support team and the junior scientists on-board, enabling the PI to pass on a few of the skills learnt over many years of OBS work, which are generally no longer required with the significantly lower equipment failure rate associated with more modern technology.

5.2 All other scientific equipment

All other ship-based scientific equipment functioned perfectly throughout the cruise except for one short period during the passage to the work area where all logging of underway data was interrupted due to a tripped mains power breaker. However, during this time the uninterruptable power supply fitted to the marine gravimeter maintained sensor heating until the mains power could be restored, and all underway systems restarted, and logging re-established.

5.3 Ship's machinery and fitted equipment

All ship's fitted equipment and machinery functioned without issue throughout the cruise.

6. Demobilisation

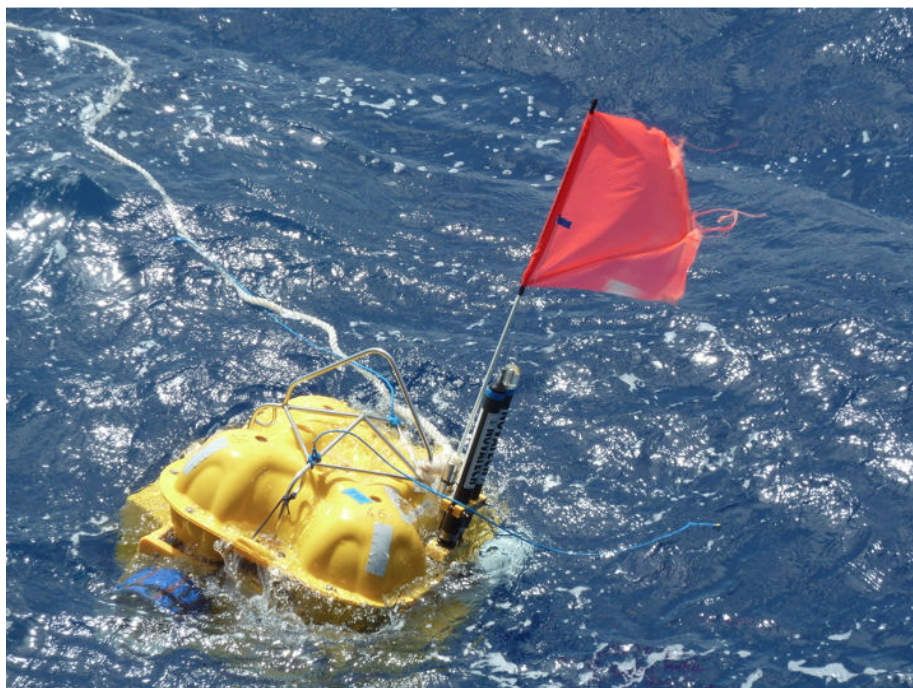
The OBS recovered during JC109 were to be used for JC114 and consequently, after demobilisation, servicing and remobilisation, all instrumentation and ancillary equipment was repacked into the 20' shipping containers loaded onto the vessel in Southampton and secured. The transit leg to Port of Spain was used for this purpose. These containers would remain on the vessel until JC114.

Acknowledgements

We would like to thank the master, deck officers, engineers and crew of the *RRS James Cook* and the support staff and sea-going technicians of NERC's National Marine Facility (NMF) for their efforts and good humour throughout this cruise. We would particularly like to thank Jez Evans, the Cruise Project Manager, whose organisation and management throughout was greatly appreciated by the scientific party. Finally, we thank Ben Pitcairn, Ian Tan and Mahshid Erfanian Mehr from the NERC's Ocean-Bottom Instrumentation Facility (OBIF) for their efficient and professional ocean-bottom instrument support. This research was funded by the U.K.'s Natural Environment Research Council under their standard grants scheme.

References

- Baines, G.B., et al., 2008. *EPSL*, **273**, 105-114.
Buck, W.R., et al., 2005. *Nature*, **434**, 719-723
Canales, J.P., et al., 2008. *G³*, **9**, Q08002
Cann, J.R. et al., 1997. *Nature*, **385**, 329-332
Cannat, M., et al., 2010. *AGU Geophys. Mono. Series*, **188**, 241-264.
Connelly, D., et al., 2011. *Nature Comms.*, **3**, 620.
deMartin, B, et al., 2007. *Geology*, **35**, 711-714.
Dick, H.J.B., et al., 2008. *G³*, **9**, Q05014.
Escartin, J. et al., 2008. *Nature*, **455**, 790-795.
Escartin, J & Canales, J-P, 2011, *EOS Trans. AGU* **92**(4), 31-32.
Grimes, C.B., et al. 2008. *G³*, **9**, Q08012.
Ildefonse, B., et al., 2007. *Geology*, **35**, 623-626.
Lavie, L.L., et al., 1999. *Geology*, **27**, 1127-1130.
MacLeod, C.J., et al., 2002. *Geology*, **30**, 879-882.
MacLeod, C.J., et al., 2009. *EPSL*, **287**, 333-344.
MacLeod, C.J., et al., 2011. *G³*, **12**, Q0AG03.
Mallows C. & Searle R., 2012, *G³*, **13**, Q0AG08.
Mallows, C. 2011. Unpubl PhD thesis, U. Durham
Morris, A., et al., 2009. *EPSL*, **287**, 217-228.
Okino, K., et al., 2004. *G³*, **5**, Q12012.
Olive, J.A., et al., 2010. *Nature Geoscience*, **3**, 491-195.
Peirce, C. & Day, A.J., 2002. *Geophys. J. Int.*, **151**, 2, 543-566.
Reston, T.J. & Ranero, C.R. 2011 *G³*, **12**, Q0AG05..
Reston TJ et al., 1999. *JGR*, **104**, 629-644.
Schouten, H., et al., 2010. *Geology*, **38**, 615-618.
Searle, R. C. et al., 2003. *G³*, **4**, 9105, doi:10.1029/2003GC000519.
Searle, R.C., et al., 2007. *RRS James Cook Cruise JC007: Cruise Report*, Durham University, 59pp.
Smith, D.K., et al., 2008. *G³*, **9**, Q03003
Tucholke, B.E. & Lin, J., 1994. *JGR*, **99**, 11,937-11,958.
Tucholke, B.E., et al., 1998. *JGR*, **103**, 9857- 9866.
Tucholke, B.E., et al., 2008. *Geology*, **36**, 455-458



Tables

Table 1 - Way points

Name	Transit and swath	(N)	(W)	Lat Deg	North Min	Long Deg	West Min	Long Deg	East Min	Long (E)
T_1		15.5000	44.0000	15	30.000	44	0.000	316	0.000	316.0000
T_2		14.7667	44.0000	14	46.000	44	0.000	316	0.000	316.0000
T_3		14.0333	44.5000	14	2.000	44	30.000	315	30.000	315.5000
T_4		13.0833	44.5000	13	5.000	44	30.000	315	30.000	315.5000
T_5		12.8500	44.0167	12	51.000	44	1.000	315	59.000	315.9833
T_6		13.4667	44.0167	13	28.000	44	1.000	315	59.000	315.9833
T_7		13.7000	44.4167	13	42.000	44	25.000	315	35.000	315.5833
T_8		14.0833	44.4167	14	5.000	44	25.000	315	35.000	315.5833
T_9		14.3333	44.3167	14	20.000	44	19.000	315	41.000	315.6833
T_10		14.7667	44.3167	14	46.000	44	19.000	315	41.000	315.6833
T_11		14.7667	44.2167	14	46.000	44	13.000	315	47.000	315.7833
T_12		13.6667	44.2167	13	40.000	44	13.000	315	47.000	315.7833
T_13		13.6667	44.3167	13	40.000	44	19.000	315	41.000	315.6833
T_14		13.9833	44.3167	13	59.000	44	19.000	315	41.000	315.6833
T_15		14.3833	44.0167	14	23.000	44	1.000	315	59.000	315.9833
T_16		14.7667	44.0167	14	46.000	44	1.000	315	59.000	315.9833
T_17		14.7667	44.1167	14	46.000	44	7.000	315	53.000	315.8833
T_18		13.6167	44.1167	13	37.000	44	7.000	315	53.000	315.8833
T_19		13.6167	44.0167	13	37.000	44	1.000	315	59.000	315.9833
T_20		14.3333	44.0167	14	20.000	44	1.000	315	59.000	315.9833
T_21		12.7000	45.3333	12	42.000	45	20.000	314	40.000	314.6667
T_22		12.7833	47.3333	12	47.000	47	20.000	312	40.000	312.6667
T_23		12.6333	48.0000	12	38.000	48	0.000	312	0.000	312.0000

TRINIDAD	Bounday between Trinidad & Tobago and Barbados waters approx..	10.7000	57.0833		10	42.000	57	4.998		302	55.002		302.9167	
ACOUSTIC	Acoustics tests	13.4300	44.8800		13	25.800	44	52.800		315	7.200		315.1200	
	OBS Deployment locations				Lat	North		Long	West		Long	East		Long
	OBS No.	(N)	(W)		Deg	Min		Deg	Min		Deg	Min		(E)
OBS_1	1	13.4065	44.8766		13	24.393	44	52.597		315	7.403		315.1234	
OBS_2	2	13.4075	44.8899		13	24.447	44	53.396		315	6.604		315.1101	
OBS_3	3	13.4074	44.9119		13	24.446	44	54.717		315	5.283		315.0881	
OBS_4	4	13.3917	44.9260		13	23.503	44	55.558		315	4.442		315.0740	
OBS_5	5	13.3915	44.9052		13	23.493	44	54.312		315	5.688		315.0948	
OBS_6	6	13.3910	44.8850		13	23.461	44	53.102		315	6.898		315.1150	
OBS_7	7	13.3906	44.8661		13	23.435	44	51.963		315	8.037		315.1339	
OBS_8	8	13.3751	44.8565		13	22.508	44	51.387		315	8.613		315.1435	
OBS_9	9	13.3765	44.8791		13	22.587	44	52.746		315	7.254		315.1209	
OBS_10	10	13.3765	44.8989		13	22.588	44	53.936		315	6.064		315.1011	
OBS_11	11	13.3780	44.9155		13	22.678	44	54.927		315	5.073		315.0845	
OBS_12	12	13.3660	44.9065		13	21.962	44	54.387		315	5.613		315.0936	
OBS_13	13	13.3620	44.8916		13	21.721	44	53.495		315	6.505		315.1084	
OBS_14	14	13.3635	44.8700		13	21.811	44	52.200		315	7.800		315.1300	
OBS_15	15	13.3570	44.8480		13	21.423	44	50.881		315	9.119		315.1520	
OBS_16	16	13.3429	44.8601		13	20.573	44	51.604		315	8.396		315.1399	
OBS_17	17	13.3483	44.8791		13	20.899	44	52.749		315	7.251		315.1209	
OBS_18	18	13.3488	44.8997		13	20.931	44	53.982		315	6.018		315.1003	
OBS_19	19	13.3548	44.9192		13	21.289	44	55.151		315	4.849		315.0808	
OBS_20	20	13.3349	44.8885		13	20.091	44	53.311		315	6.689		315.1115	
OBS_21	21	13.3290	44.8692		13	19.738	44	52.152		315	7.848		315.1308	
OBS_22	22	13.3300	44.8494		13	19.802	44	50.963		315	9.037		315.1506	
OBS_23	23	13.3128	44.8617		13	18.765	44	51.703		315	8.297		315.1383	
OBS_24	24	13.3156	44.8837		13	18.934	44	53.021		315	6.979		315.1163	
OBS_25	25	13.3010	44.8772		13	18.062	44	52.631		315	7.369		315.1228	

ADDITIONAL SWATH WAYPOINTS

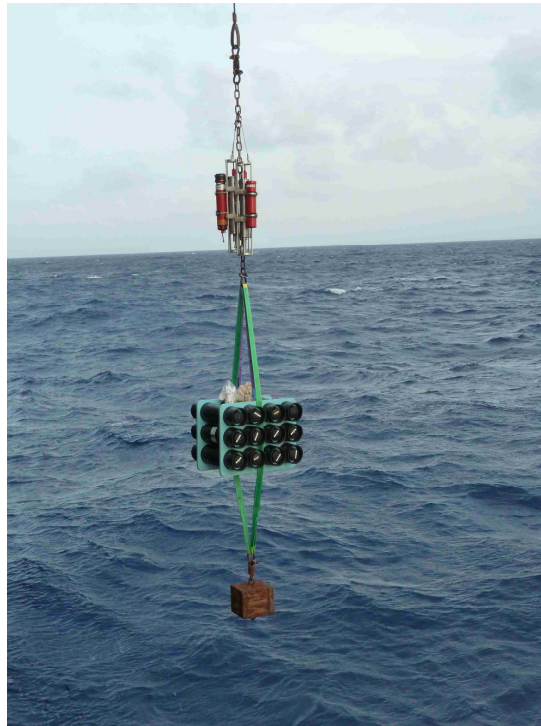
NAME	(N)	(W)	Lat Deg	North Min	Long Deg	West Min	Long Deg	East Min	Long (E)
T_24	12.5000	45.3333	12	30.000	45	20.000	314	40.000	314.6667
T_25	12.5000	45.4333	12	30.000	45	26.000	314	34.000	314.5667
T_26	12.8333	45.4333	12	50.000	45	26.000	314	34.000	314.5667
T_27	12.8333	45.5333	12	50.000	45	32.000	314	28.000	314.4667
T_28	12.5000	45.5333	12	30.000	45	32.000	314	28.000	314.4667
T_29	12.5000	45.6333	12	30.000	45	38.000	314	22.000	314.3667
T_30	13.0000	45.6333	13	0.000	45	38.000	314	22.000	314.3667
T_31	13.0000	45.7333	13	0.000	45	44.000	314	16.000	314.2667
T_32	12.5000	45.7333	12	30.000	45	44.000	314	16.000	314.2667
T_33	12.5000	45.8333	12	30.000	45	50.000	314	10.000	314.1667
T_34	13.0000	45.8333	13	0.000	45	50.000	314	10.000	314.1667
T_35	13.0000	45.9333	13	0.000	45	56.000	314	4.000	314.0667
T_36	12.5000	45.9333	12	30.000	45	56.000	314	4.000	314.0667
T_37	12.5000	46.0333	12	30.000	46	2.000	313	58.000	313.9667
T_38	13.0000	46.0333	13	0.000	46	2.000	313	58.000	313.9667
T_39	13.0167	45.9333	13	1.000	45	56.000	314	4.000	314.0667
T_40	14.3333	45.9333	14	20.000	45	56.000	314	4.000	314.0667
T_41	14.3333	46.0333	14	20.000	46	2.000	313	58.000	313.9667
T_42	13.0167	46.0333	13	1.000	46	2.000	313	58.000	313.9667
T_43	13.0000	46.1333	13	0.000	46	8.000	313	52.000	313.8667
T_44	12.5000	46.1333	12	30.000	46	8.000	313	52.000	313.8667
T_45	12.5000	46.2333	12	30.000	46	14.000	313	46.000	313.7667
T_46	13.0000	46.2333	13	0.000	46	14.000	313	46.000	313.7667
T_47	13.0167	46.1333	13	1.000	46	8.000	313	52.000	313.8667
T_48	14.3333	46.1333	14	20.000	46	8.000	313	52.000	313.8667

Table 2 - OBS recovery locations

OBS No.	(N)	(W)	Deg	Min (N)	Deg	Min (W)	Deg	Min	(E)
1	13.4093	44.8805	13	24.560	44	52.830	315	7.170	315.1195
2	13.4053	44.8932	13	24.320	44	53.590	315	6.410	315.1068
3	13.4067	44.9150	13	24.400	44	54.900	315	5.100	315.0850
4	13.3917	44.9300	13	23.500	44	55.800	315	4.200	315.0700
5	13.3883	44.9100	13	23.300	44	54.600	315	5.400	315.0900
6	13.3900	44.8867	13	23.400	44	53.200	315	6.800	315.1133
7	13.3887	44.8703	13	23.320	44	52.220	315	7.780	315.1297
8	13.3750	44.8583	13	22.500	44	51.500	315	8.500	315.1417
9	13.3760	44.8813	13	22.560	44	52.880	315	7.120	315.1187
10	13.3750	44.9017	13	22.500	44	54.100	315	5.900	315.0983
11	13.3767	44.9183	13	22.600	44	55.100	315	4.900	315.0817
12	13.3633	44.9150	13	21.800	44	54.900	315	5.100	315.0850
13	13.3617	44.8942	13	21.700	44	53.650	315	6.350	315.1058
14	13.3617	44.8733	13	21.700	44	52.400	315	7.600	315.1267
15	13.3550	44.8517	13	21.300	44	51.100	315	8.900	315.1483
16	13.3527	44.9138	13	21.160	44	54.830	315	5.170	315.0862
17	13.3467	44.8817	13	20.800	44	52.900	315	7.100	315.1183
18	13.3483	44.9033	13	20.900	44	54.200	315	5.800	315.0967
19	13.3533	44.9217	13	21.200	44	55.300	315	4.700	315.0783
20	13.3333	44.8900	13	20.000	44	53.400	315	6.600	315.1100
21	13.3283	44.8733	13	19.700	44	52.400	315	7.600	315.1267
22	13.3283	44.8533	13	19.700	44	51.200	315	8.800	315.1467
23	13.3117	44.8667	13	18.700	44	52.000	315	8.000	315.1333
24	13.3150	44.8883	13	18.900	44	53.300	315	6.700	315.1117
25	13.2983	44.8817	13	17.900	44	52.900	315	7.100	315.1183

Table 3 - Sound velocity profile and acoustic tests

	Day	Time GMT	Latitude (N) Deg	Min	Longitude (W) Deg	Min
Acoustic tests and Sound velocity profile	299	17:22	13	25.76	44	52.97



Sound velocity probes (silver) and USBL transponders (red) attached above the OBS acoustic release carousel.

Table 4 - Gravity base stations

	Latitude (N) Deg	Min	Longitude (W) Deg	Min
Absolute gravity base station NOC, Southampton (location taken from the station's data sheet, lat/long suspect)	50	53.5000	1	23.6000
Quayside <i>RRS Cook</i> – pre-cruise, adjacent to NOC, Southampton	50	53.8278	1	23.6908
SE corner customs warehouse, Port of Spain	10	39.1217	61	31.1817
Quayside <i>RRS Cook</i> – post-cruise Between bollard 27 and 28 Midway, on join in concrete slab 2.05m from quay edge	10	39.1167	61	31.1826

Table 5 - Scientific personnel

The RRS James Cook carried a total crew of 30 people for cruise JC109 as named below:

Master	Andrew Smith
Chief Officer	Philip Gauld
2 nd Officer	Declan Morrow
3 rd Officer	Paul Brown
Chief Engineer	George Parkinson
2 nd Engineer	Michael Murray
3 rd Engineer	Michael Murren
3 rd Engineer	Lawrence Porrelli
ETO	Sebastian Ulbrecht
ERPO	Brian Conteh
CPO(Science)	Martin Harrison
CPO (Deck)	Philip Allison
PO (Deck)	David Price
Seaman	Mark Moore
Seaman	Jarrod Welton
Seaman	David Mackenzie
Seaman	Nicholas Byrne
Purser	Anthony Stevens
Head Chef	Darren Caines
Chef	Christopher Keithley
Steward	Peter Robinson
Assistant Steward	Kevin Mason
Principal Scientist	Christine Peirce
Scientist	Matthew Funnell
Scientist	Adam Robinson
OBS Technical Support (Lead)	Ben Pitcairn
OBS Technical Support	Ian Tan
OBS Technical Support	Mahshid Erfanian Mehr
Technical Liaison Officer	Martin Bridger
Technical Support	Andrew Moore

Table 6 - Project 13N Principal Scientists, Project Partners and Consultants

The Principal Scientists, Project Partners and Consultants for the *13N MAR* project are:

Principal Scientists:	Professor Tim Reston (Birmingham University) Professor Christine Peirce (Durham University) Professor Chris MacLoed (Cardiff University)
Project Partners:	Dr Robert Sohn (Woods Hole Oceanographic Institution) Dr Juan Pablo Canales (Woods Hole Oceanographic Institution) Dr Javier Escartin (Institute de Physique de Globe, Paris)
Consultants:	Professor Roger Searle (Emeritus, Durham University) Professor Joe Cann (Emeritus, Leeds University)